

## Review Article

# A Review on Synthesis and Characterization of Ag<sub>2</sub>O Nanoparticles for Photocatalytic Applications

Workneh M. Shume , H. C. Ananda Murthy , and Enyew Amare Zereffa 

*Department of Applied Chemistry, School of Applied Natural Science, Adama Science and Technology University, Adama, Ethiopia*

Correspondence should be addressed to Workneh M. Shume; [worknehme@gmail.com](mailto:worknehme@gmail.com) and H. C. Ananda Murthy; [anandkps350@gmail.com](mailto:anandkps350@gmail.com)

Received 20 December 2019; Accepted 16 March 2020; Published 1 June 2020

Academic Editor: David E. Chavez

Copyright © 2020 Workneh M. Shume et al. This is an open access article distributed under the Creative Commons Attribution License, which permits unrestricted use, distribution, and reproduction in any medium, provided the original work is properly cited.

Even though the photocatalytic processes are a good technology for treatment of toxic organic pollutants, the majority of current photocatalysts cannot utilize sunlight sufficiently to realize the decomposition of these organic pollutants. As stated by various researchers, metal oxide nanoparticles have a significant photocatalytic performance under visible light source. Among various chemical and physical methods used to synthesize nanostructured silver oxide, green synthetic route is a cheaper and environmental friendly method. To confirm the optimum production of Ag<sub>2</sub>O NPs, effect of pH, extract concentration, metal ion concentration, and contact time were optimized. The structure, morphology, crystallinity, size, purity, elemental composition, and optical properties of obtained Ag<sub>2</sub>O NPs were characterized by different techniques, such as scanning electron microscopy (SEM), transmission electron microscope (HRTEM), X-ray diffraction (XRD), energy dispersive spectroscopy (EDS), X-ray photoelectron spectroscopy (XPS), Fourier transform infrared spectroscopy (FT-IR), and UV-visible spectrophotometer accordingly as revealed by our literature review. The photocatalytic performance of the synthesized nanocrystalline Ag<sub>2</sub>O by photocatalytic degradation of organic dyes under visible light irradiation has been discussed thoroughly in this review. Many past studies revealed that organic dyes and pollutants are decomposed completely by green synthesized Ag<sub>2</sub>O NPs under irradiation of visible light.

## 1. Introduction

Sixty years ago, December 29, 1959, the best known paper of nanotechnology entitled “There’s Plenty of Room at the Bottom” was delivered by physicist Professor Richard Feynman to the American Physical Society at the California Institute of Technology, Pasadena [1]. In the paper, Professor Richard Feynman described the possibilities, if we could learn to control single atom and molecules. The work led the community to the era of nanotechnology. Hence, the essence of nanotechnology is based on the ability to work at the molecular and atomic levels to formulate fundamentally new molecular structure with advance physicochemical properties [2]. The combination of science and technology for the nature of material at the nanoscale provides a strong foundation for nanotechnology [3]. The products based on

nanotechnology are currently on the market of which the majority are incorporated in everyday personal-care products, cosmetics, and clothing.

In the recent years, the nanomaterials have received great attention from the scientific community not only because of their fascinating properties but also due to their many technological applications [2]. Behavior of materials at the nanoscale as compared to macroscale often is found to be highly desirable properties which are created due to size confinement, the dominance of interfacial phenomena, and quantum effects [2]. These new and unique properties of nanostructured materials lead to improved properties such as catalysts, tunable photo activity, increased strength, and many other interesting characteristics. It plays a major role in the development of innovative methods to produce new products, to substitute existing production equipment and

to reformulate new materials and chemicals with improved performance resulting in less consumption of energy and materials and reduced harm to the environment as well as environmental remediation [3].

Environmental applications of nanotechnology address the development of solutions to the existing environmental problems, preventive measures for future problems resulting from the interactions of energy and materials with the environment, and any possible risks that may be posed by nanotechnology itself.

The use of pesticides, herbicides, solvents, organic dyes, and so forth rapidly in agriculture and large scale industrial (such as food, pharmacy, cosmetics, paints, plastics, paper, and textiles) development activities are causing much trouble and concern for the scientific communities and environmental regulatory authorities around the world. Due to their toxicity and persistence these organic pollutants adversely affect the environment and human health and are a major source of aesthetic pollution, eutrophication, and ecological disturbance in aquatic life. To safeguard of our environment, it is very important to detoxify these hazardous organic pollutants. Because of their aromatic structural stability it is difficult to remove by techniques such as coagulation, filtration, reverse osmosis, and adsorption: nowadays many scientists suggested photocatalytic process is one of the promising methods for the detoxification of various toxic and hazardous pollutants as well as remedies of environment [4].

In recent years, extensive research has shown the metal oxide semiconductors based photocatalysts with wide potential applications in environmental purification and solar energy conversion have drawn a wide public attention [5]. Several metal oxides such as  $\text{Ag}_2\text{O}$ ,  $\text{TiO}_2$ ,  $\text{ZnO}$ ,  $\text{MoO}_3$ ,  $\text{ZrO}_2$ ,  $\text{WO}_3$ ,  $\alpha\text{-Fe}_2\text{O}_3$ ,  $\text{SnO}_2$ , and  $\text{SrTiO}_3$  and some chalcogenide metals ( $\text{ZnS}$ ,  $\text{CdS}$ ,  $\text{CdSe}$ ,  $\text{WS}_2$ , and  $\text{MoS}_2$ ) have been applied as photocatalysts which is an area of intensive research [6]. Nanometal oxides have major applications investigated in photocatalysis technology for color removal and destruction of persistent organic pollutants, especially dyes that constitute the largest group of hazardous organic compounds and increasing environmental danger [7]. Narrow band gap semiconductors (e.g.,  $\text{Ag}_2\text{O}$ ,  $\text{CuO}$ , and  $\text{ZnO}$ ) can absorb full solar spectrum of light and a high photocatalytic application [8]. Silver oxide ( $\text{Ag}_2\text{O}$ ) nanoparticles with a direct band gap of 1.2 eV is a kind of p-type semiconductors [5, 9], which is a very strong decoloring agent used as photocatalytic degradation of organic pollutants in water [10–13].

Over the past decade, a variety of chemical and physical methods have been employed for the synthesis of  $\text{Ag}_2\text{O}$  with different morphologies for different applications [14]. However, the physical and chemical methods are hazardous, toxic, and expensive [10]. Hence, the scientific community has turned their attention towards low cost, nontoxic, simple, and ecofriendly synthesis of silver oxide nanoparticles from biological sources like plants fungi and microbes [10].

This review presents the importance of  $\text{Ag}_2\text{O}$  nanoparticles with main focus to photocatalytic application for the degradation of organic dyes. Here, we discussed various

synthetic routes and characterization techniques employed to get morphological, structural, optical, and electrical properties of  $\text{Ag}_2\text{O}$  NPs. In addition to these, the stability and repeated photocatalytic efficiency of the  $\text{Ag}_2\text{O}$  photocatalyst were also discussed.

*1.1. Green Synthetic Methods of Nanoparticle.* Many of the chemical and physical methods used for the synthesis of metal oxide nanoparticles are too expensive and also involve the use of toxic, hazardous chemicals as reducing and stabilizing agent, which are accountable for various biological risks. This enhances the growing need to develop environment friendly processes through green synthesis and other biological approaches [2]. Those, due to their cost-effectiveness, environmental friendly nature and easy handling, green synthesis processes are regarded as safer alternative to usual physical, chemical, and microbial methods. Development of environmental friendly and green processes for synthesis of noble metal oxide nanoparticles is evolving into an important branch of nanotechnology [4]. For the development of green chemistry, three main factors in nanoparticle preparation should be considered: (i) selection of solvent medium, (ii) selection of environmentally benign reducing agents, and (iii) selection of nontoxic materials for nanoparticle stabilization [2]. Based on this approach, green synthetic method becomes more advisable for the synthesis of metal oxide nanoparticles.

*1.2. Photocatalysis Processes and Mechanism.* Catalysts are utilized for speeding up the chemical reaction and, similarly, a photocatalyst employs the catalyst for speeding up chemical reactions in the presence of UV-visible light [15]. Photocatalytic reactions provide suitable way to promote the separation of molecular hydrogen and molecular oxygen from water using solar illumination [16]. These types of reactions are activated by absorption of light with sufficient energy (equal to or higher than the band gap energy ( $E_{bg}$ ) of the photocatalyst. The absorption of light leads to generating a hole ( $h^+$ ) in the valence band a charge separation due to promotion of an electron ( $e^-$ ) from the valence band to the conduction band of the semiconductor catalyst; thus, the schematic diagram of the process is presented in Figure 1 [15, 17].

The oxidation and reduction reactions on the surfaces of photocatalyst material, mediated by the valence band (VB) holes ( $h^+$ ) and conduction band (CB) electrons ( $e^-$ ) generated by the absorption of UV-visible light radiation, refer to photocatalysis. Such photogenerated pairs of  $h^+$  and  $e^-$  induce the formation of aggressive species ( $\text{OH}^-$  ions and superoxide radicals) which are strong enough to oxidize and decompose or mineralize harmful organic pollutants [5, 8, 18, 19].

*1.3. Silver Oxide ( $\text{Ag}_2\text{O}$ ).* Silver oxide is well-known semiconductor metal oxide having vast applications: in the field of electrochemical, electronic, optical properties [20], oxidation catalysis, sensors, fuel cells, photovoltaic cells, all-

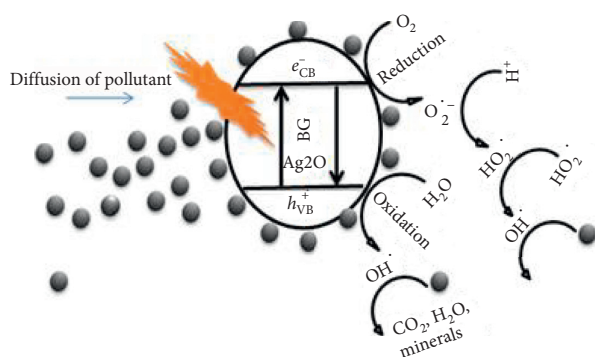


FIGURE 1: Schematic representation of photocatalytic mechanism.

optical switching devices, optical data storage systems, and as a diagnostic biological probes, [21] anticancer chemotherapy, antibiotics, and cosmetics [10–13]. In recent year due to its high catalytic activity, and selectivity,  $\text{Ag}_2\text{O}$  nanoparticles become one of the most popular photocatalysts.

Recently, notable progress in the photocatalysis process is the observation of silver-containing photocatalysts, such as  $\text{Ag}_2\text{O}$ ,  $\text{Ag}_3\text{PO}_4$ ,  $\text{Ag}_3\text{VO}_4$ , and  $\text{Ag}_2\text{CO}_3$ , which exhibit excellent photocatalytic activity in degrading persistent organic pollutant in contrast to the other visible light driven photocatalysts such as  $\text{N-TiO}_2$ ,  $\text{BiVO}_3$ , and  $\text{Zn}_2\text{S}$  [7].

Silver oxide nanoparticle possessing a simple cubic structure with a lattice parameter of 0.472 nm has been widely used in many industrial fields, as cleaning agents, preservatives, colorants, electrode materials, and catalysts for alkane activation and olefin epoxidation [22].

## 2. Nanosynthetic Approach and Optimization

**2.1. Synthesis of  $\text{Ag}_2\text{O}$  Nanoparticles.** Synthesis of  $\text{Ag}_2\text{O}$  NPs is of much interest to the scientific community because of their wide range of applications. Stable silver oxide nanoparticles can be synthesized by using physical methods (vapor deposition, sonochemical, and so forth), chemical methods (chemical reduction, sol gel, chemical vapor deposition, coprecipitation method, and so forth) and biosynthetic methods (using naturally obtained material like plants, bacteria, fungi, or microbial organisms as a source of capping or stabilizing agent instead of chemicals). All these methods meet the requirements of different nanoparticle-mediated applications. As reported by earlier researchers, since the physical and chemical methods are used hazardous chemicals as a reducing and stabilizing agent, which make them toxic and expensive, due to this reason researchers attract their attention towards nontoxic, cost-effective, and simple methods which is called biosynthesis method.

Green synthesis (biosynthesis) method used for obtaining nanoparticles via naturally occurring reagents such as vitamins, sugars, plant extracts, biodegradable polymers, and microorganisms as reductants and capping agents could be considered attractive for nanotechnology. The advancement of green synthesis over chemical and physical methods is environment friendly, cost-effective, and

easily scaled up for large scale syntheses of nanoparticles; furthermore there is no need to use high temperature, pressure, energy, and toxic chemicals [23]. A lot of literature has been reported till date on biological syntheses of silver oxide nanoparticles using microorganisms including bacteria, fungi, and plants because of their antioxidant or reducing properties typically responsible for the reduction and stabilizing of metal compounds in their respective nanoparticles. Among them plant based materials seem to be the best candidates and they are suitable for large scale “biosynthesis” of nanoparticles. Plant parts such as leaf, root, latex, seed, and stem are being used for silver oxide nanoparticle synthesis. It is the best platform for synthesis of nanoparticles, being free from toxic chemicals as well as providing natural capping agents for the stabilization of nanoparticles. A lot of researchers have synthesized  $\text{Ag}_2\text{O}$  NPs by using various types of plant sample for different applications.  $\text{Ag}_2\text{O}$  NPs were synthesized by using *Artocarpus heterophyllus* (Jackfruit tree) for antibacterial activity against dental pathogens [10];  $\text{Ag}_2\text{O}$  NPs were synthesized by using *Cubes to Octapods* for antibacterial application [11];  $\text{Ag}_2\text{O}$  NPs were synthesized by using *aqueous leaf extract of Callistemon lanceolatus* (Myrtaceae) [24];  $\text{Ag}_2\text{O}$  NPs were synthesized by using *Waste Part of Mango Peels* [25];  $\text{Ag}_2\text{O}$  NPs were synthesized by using *Garcinia mangostana Fruit Extract* for antibacterial and antioxidant application [14];  $\text{Ag}_2\text{O}$  NPs were synthesized by using *Carica papaya Root Extract* [12], and  $\text{Ag}_2\text{O}$  NPs were synthesized by using *Ficus benghalensis prop root extract* (FBPRE) for the ecofriendly synthesis of silver oxide nanoparticles [10]. It has been very well accepted by the recent scientific researchers that green synthesis can be a better alternate method of synthesis of nanoparticles compared to other physical and chemical methods owing to its simplicity, nontoxic nature, and environment friendly nature.

**2.1.1. Synthesis and Optimization of Silver Oxide Nanoparticles.** The reduction and stabilization of silver ions by combination of biomolecules such as proteins, amino acids, enzymes, polysaccharides, alkaloids, tannins, phenolics, saponins, terpenoids, and vitamins which are already established in the plant extracts having medicinal values and are environmental benign, yet chemically complex structures [26]. Many species of plants were reported to facilitate synthesis of  $\text{Ag}_2\text{O}$  NPs. The protocol for the nanoparticle syntheses involves the collection of the part of plant of interest from the available sites and then washing thoroughly twice/thrice with tap water to remove both epiphytes and necrotic plants, followed with sterile distilled water to remove associated debris if any. These clean and fresh sources are shade-dried for 10–15 days and then powdered using domestic blender. For the plant broth preparation, around 100 g of this powder was added to 250 mL of deionized water in a flask, mixed well, and maintained on a magnetic heating stirrer. The resulting infusion is then filtered thoroughly with Whatman filter paper until no insoluble material appeared. The pure  $\text{AgNO}_3$  (99.9%) to 1 mM dissolved in aqueous solution as the metal precursor.

To obtain silver oxide nanoparticles ( $\text{Ag}_2\text{O}$  NPs), a few mL of extracted sample was added to 1 mM of silver nitrate solution in Erlenmeyer flasks to form a reaction mixture, and the reaction performed under ambient conditions. Initial confirmation of silver nanoparticle production is insured by change in color from light yellow to dark brown in the reaction mixture following the reduction of pure  $\text{Ag}(\text{I})$  ions to  $\text{Ag}(0)$  which can be monitored by measuring the UV-visible spectra of the solution at regular intervals (Figure 2) [10–12, 14, 26, 28].

(1) *Optimize the Nanoparticle Production.* The parameters such as pH, ratio of  $[\text{Ag}^+]$  to extracted sample, and a time frame were tested (Figure 3). Once the production of silver oxide nanoparticle, optimized by using parameters stated above, centrifuged the obtained product for a certain minutes, followed by several washes with copious amounts of pure water and ethanol to ensure separation of free entities from the silver nanoparticles [10, 12, 14, 26, 28], the plant extract-mediated synthesis of silver nanoparticles hypothesized that the presence of bioactive compounds, such as polyphenols (flavonoids) has hydroxyl and ketonic groups that bind to the bulk metal silver ion reduce it to nanosize [10]. The formation of  $\text{Ag}_2\text{O}$  nanoparticles could be mediated by the presence of  $\text{OH}^-$ . This contributes the  $\text{OH}^-$  group to  $\text{Ag}^+$  and results in the formation of highly unstable  $\text{AgOH}$ , which is readily oxidized to  $\text{Ag}_2\text{O}$  by freeze-drying [24].

2.1.2. *Photocatalytic Experiment.* The photocatalytic performance of  $\text{Ag}_2\text{O}$  NPs by using different organic dyes and pollutants has been explored by the past researchers. The photocatalytic activity of  $\text{Ag}_2\text{O}$  NPs has been evaluated by decolorization of aqueous organic dyes and pollutants. The photocatalytic activity of the green synthesized samples for decolorization of aqueous solutions of organic dyes and pollutants was performed at ambient temperatures.

The synthesized  $\text{Ag}_2\text{O}$  powder was dispersed in an organic dyes or pollutants solution, prepared by dissolving the organic powders in deionized water in a test tube. At room temperature, the test tube was placed on the support standing in the darkroom of photo reactor system. A visible light was used as a light source. Before irradiation, the suspensions were magnetically stirred in the dark for a certain time (usually more than 40 min) to ensure the establishment of adsorption–desorption equilibrium of dyes on the sample surfaces. The average light intensity striking the surface of the reaction solution should be bright enough. After irradiation, suspensions including the sample powders and dyes were sampled from the same tube every few seconds. Then the sample powders were separated by centrifuging, and the clarified dye solutions were analyzed with a UV-Vis spectrophotometer to determine the concentration of the organic dyes by monitoring the height of the maximum of the absorbance peak in ultraviolet–visible spectra of the solution [7, 24].

The percentage of organic pollutant degradation can be calculated by

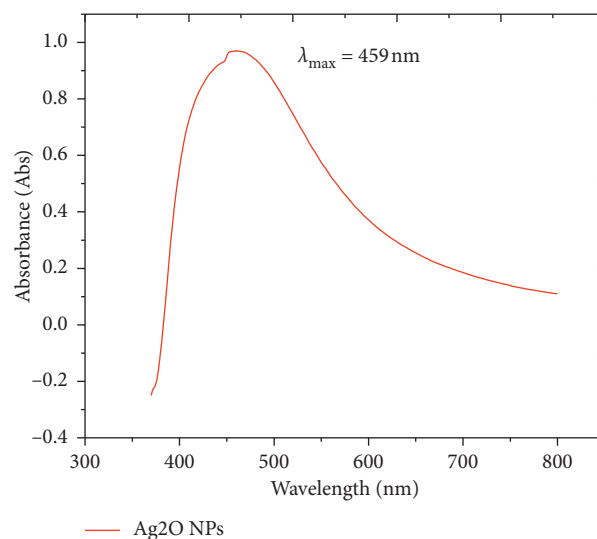


FIGURE 2: UV-Vis adsorption spectra of  $\text{Ag}_2\text{O}$  NPs [27].

$$\text{degradation rate (\%)} = \frac{A - B}{A} \times 100, \quad (1)$$

where  $A$  is the total of pollutants obtained without  $\text{Ag}_2\text{O}$  NPs and  $B$  is the amount of pollutants with  $\text{Ag}_2\text{O}$  NPs. Consequently,  $D$  (%) is the percentage of degradation, which indicates the photocatalytic efficiency [10, 28].

2.2. *Characterization Techniques.* Nanoscale materials often present properties different from their bulk counterparts, as their high surface-to-volume ratio results in an exponential increase of the reactivity at the molecular level. Such properties include electronic, optical, and chemical properties, while the mechanical characteristics of the nanoparticles (NPs) may also differ extensively. Several techniques are available for the characterization of stable metal oxides nanoparticles such as UV-Vis spectroscopy, Fourier transform infrared spectroscopy (FTIR), X-ray diffraction technique (XRD), thermogravimetric analysis (TGA), scanning electron microscopy (SEM), energy dispersive X-ray spectroscopy (EDX), electron energy loss spectroscopy (EELS), transmission electron microscopy (TEM), and atomic force microscopy (AFM).

Among the various characterization techniques mentioned in Figure 4, a brief description of the techniques for characterization of green synthesized silver oxide nanoparticle used in this work as reported by several scholars has been presented below.

2.2.1. *UV-Visible Spectral Technique.* The Ultraviolet-visible (UV-Vis) absorption spectroscopy is a valuable technique for the characterization of the absorbance bands and band gap of nanoparticles (DRS) especially that of noble metals because they are intensely colored and show absorptions due to surface plasmon oscillations. Surface plasmon is the light waves that are trapped on the surface because of their interaction with the free electrons of the metal. It should be noted that the SPR band is characteristic of metal

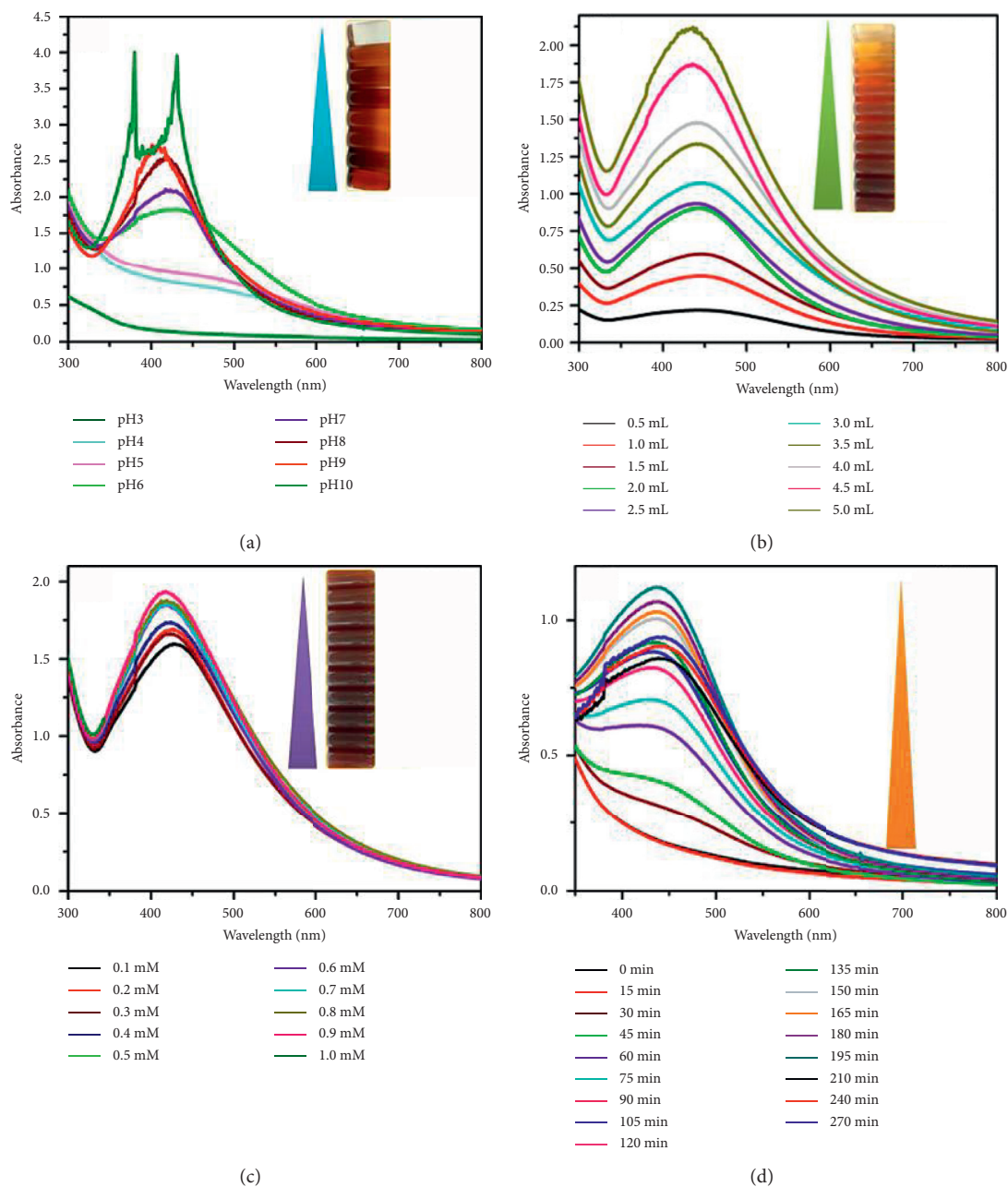


FIGURE 3: UV-Vis absorption spectra-optimization of parameters for the production of Ag<sub>2</sub>O NPs with different pH (a), plant extract from 0.5 to 5 mL (b), concentration of metal ions Ag<sup>+</sup> from 0.1 to 1.0 mM (c), and different times from 0 to 270 min (d) [10].

nanoparticles and is not observed in the spectrum of their bulk counterparts [3].

For characterization of Ag<sub>2</sub>O NPs many literatures commonly used UV-visible spectrophotometer in the range 300–800 nm with a resolution of 1 nm at room temperature. In general, the absorption maxima depend on the particle size of Ag<sub>2</sub>O NPs. In case of absorption of visible light, colors of the NPs were found to differ. The analysis was carried out with quartz cuvettes as sample container [29]. The reaction mixture was monitored spectrophotometrically at every 30 min interval from 0 to 150 min [10].

**2.2.2. Fourier Transform Infrared Spectroscopic (FT-IR) Technique.** Fourier transform infrared (FTIR) spectrophotometer is used to detect functional groups involved in synthesized nanoparticle at a resolution of 4 cm<sup>-1</sup> in a diffuse reflectance mode and using KBr pellets [10]. Potassium bromide pellets were prepared for each extract and the nanoparticles. This technique helps us to determine which bonds are responsible from the synthesis and the stability of the silver oxide nanoparticles [24]. For the analysis, the powdered nanoparticle sample was mixed with KBr pellets (FT-IR grade). The pellet was placed into the sample holder

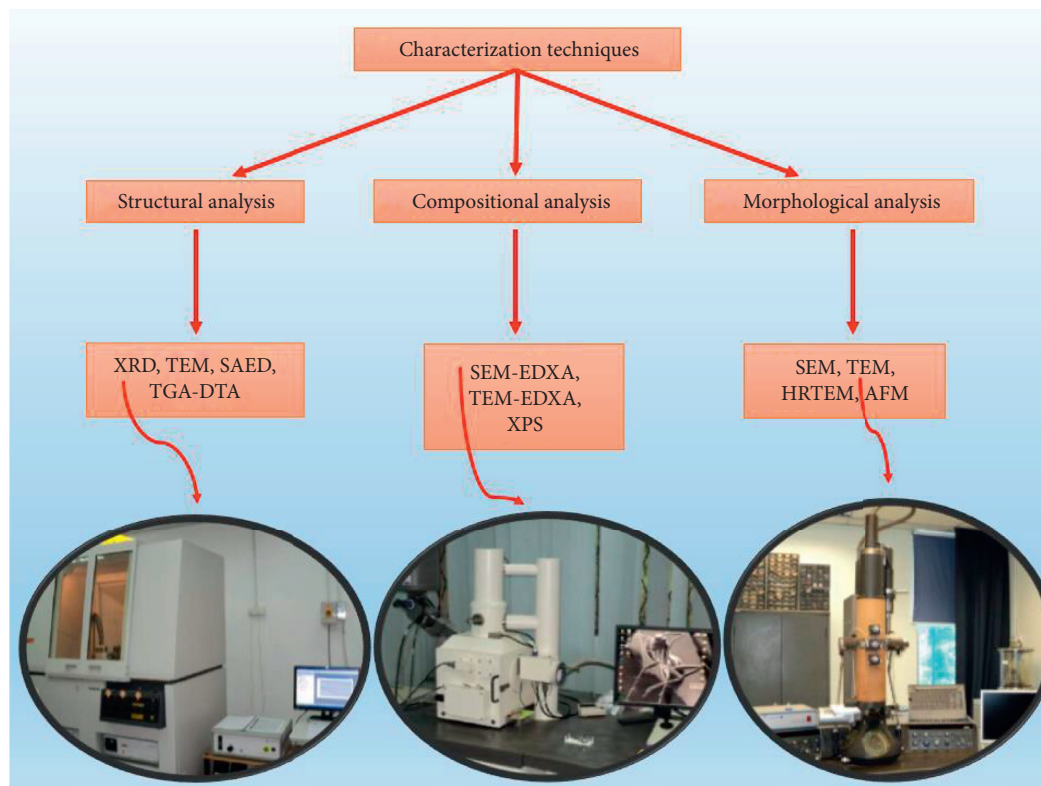


FIGURE 4: General techniques available for the characterization of nanoparticles.

and FT-IR spectra were recorded in the range  $4000\text{--}500\text{ cm}^{-1}$  in FT-IR spectroscopy [10].

**2.2.3. X-Ray Diffraction (XRD) Techniques.** The X-ray diffraction (XRD) spectrum is used to confirm the crystalline nature of the synthesized silver oxide nanoparticle. The powdered sample is placed on a glass slide and subjected to XRD analysis taken with a computer controlled [10]. Analysis was carried out over a  $2\theta$  scale of  $30\text{--}80$  degrees at a scan rate of  $0.5$  degrees/min. The resultant data was analyzed using Match Software [10, 30].

**2.2.4. Scanning Electron Microscope-Energy Dispersive X-Ray (SEM-EDX) Technique.** SEM is used for more detailed morphological studies [29]. After the color change of the reaction mixture during the synthesis of  $\text{Ag}_2\text{O}$  NPs, a drop of nanoparticle suspension was placed on aluminium coated SEM grid and analyzed under an SEM instrument coupled with EDX detector [24].

**2.2.5. High-Resolution Transmission Electron Microscope (HRTEM) Technique.** High-resolution transmission electron microscopy and selected area electron diffraction (SAED) pattern are used to examine the morphology, size, and crystallinity of the  $\text{Ag}_2\text{O}$  NPs [10]. Ultrathin film of green synthesized  $\text{Ag}_2\text{O}$  NPs is prepared on a carbon coated copper grid. For the analysis, a drop of suspension containing the nanoparticles was placed on a carbon coated TEM grid in a vacuum desiccator and subsequently analyzed using HRTEM instrument [24].

**2.2.6. X-Ray Photoelectron Spectroscopy (XPS).** XPS is a spectroscopic technique used to identify the elemental composition, valance state, and purity of the synthesized silver oxide nanoparticle. XPS spectrum of  $\text{Ag}_2\text{O}$  NPs is obtained in the range of  $0\text{--}1350$  eV [28].

**2.2.7. Energy Dispersive Spectroscopy (EDS) Techniques.** EDS is a spectroscopic technique used to identify the elemental composition and purity of the synthesized  $\text{Ag}_2\text{O}$  NPs. EDS spectrum of silver oxide nanoparticle is obtained in the range of  $0\text{--}1350$  eV [28].

### 3. Characterization of Synthesized Silver Oxide Nanoparticles

The  $\text{Ag}_2\text{O}$  NPs prepared by a green synthesis method with silver nitrate and a few mL of plant extract have been characterized by various techniques such as UV-visible, FT-IR, DRS, XRD, TEM/HRTEM/SAED, SEM, EDAX, and XPS before its application as photocatalyst for the decomposition of the persistent organic pollutant.

**3.1. Optimization Parameters.** Figures 3(a)–3(d) show a strong absorption band over  $430$  nm within the graph of all parameters which confirmed a surface plasmon resonance peak (SPR), corresponding to the production of silver oxide NP [12, 31]. These results are in good agreement with earlier findings of Velu et al., who studied the production, optimization, and characterization of  $\text{Ag}_2\text{O}$  NPs using *Artocarpus heterophyllus* rind extract [27]. The obtained peaks

were found to match very well with results obtained from Ag<sub>2</sub>O NPs synthesized by chemical and physical methods. This confirmed that the green synthesis method is also an efficient method for the synthesis Ag<sub>2</sub>O NPs.

As shown in Figures 3(a)–3(d) as reported by Manikandan a maximum production of Ag<sub>2</sub>O NPs resulted at the optimal conditions of pH 9, 5 mL of plant extract, 0.9 mM Ag<sup>+</sup> solution, and time frame 195 min [10].

In general, results observed on Figure 3 strongly suggested that the parameters like the concentration of hydrogen ion, the concentration of bioactive compounds present in plant extract, the concentration of metal precursors and the incubation period were found to play a key role in the formation of Ag<sub>2</sub>O NPs.

UV-visible spectroscopy is a convenient tool for measuring the reduction of metal ions based on optical properties called SPR. As shown in Figure 3 the UV-visible spectrum of silver oxide nanoparticles clearly exhibits a wider absorption in the whole UV-visible light region of 200–800 nm [10]. A strong absorption band over 430 nm shows a surface plasmon resonance peak (SPR), suggesting the formation of Ag<sub>2</sub>O NPs [27]. This hypothesized that the bioactive compounds present in the plant extract, such as polyphenols (flavonoids), have hydroxyl and ketonic groups that bind to the bulk metal silver to reduce it to nanosize [10].

**3.2. Energy Band Structure of Ag<sub>2</sub>O NPs.** The band gap energy is a key property influencing the photocatalytic performance of the photocatalyst. The band gap value of Ag<sub>2</sub>O was reported to be 1.2 eV to 1.43 eV [5, 9]. The absorbance edge could not be determined directly in the whole measured light region. If the tangent line of the absorption curve was extended, the absorption edge could be estimated as >800 nm by the crossing point of tangent line and *x*-axis. The corresponding band gap value of Ag<sub>2</sub>O could be estimated according to the equation:

$$E_g = \frac{1240}{\lambda_g}, \quad (2)$$

where  $E_g$  is the band gap of the semiconductor and  $\lambda_g$  is the threshold wavelength, the wavelength of the corresponding absorbance edge [7].

**3.3. Surface Chemistry.** The stabilizing or capping agents attached to the metal nanoparticle surface show FTIR pattern which is different from those of free groups. FTIR is a technique based on the vibrations of atoms within a molecule. Hence, FTIR gives information about the surface chemistry of Ag<sub>2</sub>O NPs [32].

The surface chemistry analysis of the major functional groups in water extract control and their possible involvement in the synthesis of silver oxide nanoparticle were characterized with the help of FTIR in the range between 4000 and 500 cm<sup>-1</sup> (Figure 5). The FT-IR absorptions spectrum of water extract control and silver oxide NPs was shown at 3438 cm<sup>-1</sup> representing stretching vibration of alcohol (OH group); 2931 cm<sup>-1</sup> assigned to the stretching

vibration of C-H methyl and methylene bond; 1613 cm<sup>-1</sup> assigned to the C=O stretching of pectin ester and carboxylic acid and so on [10].

These results are in agreement with various studies of biologically synthesized Ag<sub>2</sub>O NPs using *Artocarpus heterophyllus* (Jackfruit tree) [10], *Octapods* [11], *Callistemon lanceolatus* (Myrtaceae) [24], *Waste Part of Mango Peels* [25], and *Carica papaya Root Extract* [12]. The shifting of FTIR spectral peaks (Figure 5) corresponding to the major functional group as compared with obtained silver oxide NPs is an indication of the major biomolecules are responsible for the reduction of Ag<sup>+</sup> to Ag<sup>0</sup>, by capping on the Ag<sub>2</sub>O NPs surface.

According to the reported studies the metal–oxygen stretching frequencies normally appear at the range of 500 to 600 cm<sup>-1</sup> [24]. Thus, in Figure 5 the weak band obtained at 588.29 cm<sup>-1</sup> attributed to the Ag–O vibration includes those for crystal (lattice) and coordinated water as well as Ag<sub>2</sub>O. The asymmetric and symmetric stretching H–O–H vibration bands are observed at 3,100 cm<sup>-1</sup>. Other bands can be attributed to silver nitrate and the phytochemical constituents of the leaf extract [24].

**3.4. Crystal Structure.** The crystal structure of the Ag<sub>2</sub>O NPs was first established as the cubic structure type with a measured lattice constant of 4.728 Å in 1912 [30]. Later, more accurate crystal structures were established as a result of progress in X-ray diffraction techniques. X-ray diffraction is a nondestructive technique used for the identification of crystal structure and purity of nanoparticles. Each crystalline solid has unique atomic structure and has a characteristic X-ray diffraction pattern. These patterns can be used as fingerprints for the identification of the crystal structure [33]. The results of many studies reported in literature suggested as the biosynthesized silver oxide NPs have two basic crystalline structures (cubic and face center). The XRD patterns (Figure 6) of biosynthesized silver oxide reported on different studies show two intense peaks at 2θ values of 20.06°–38°, which corresponds to (110) and (111) of Ag<sub>2</sub>O. Apart from these diffraction peaks observed at 40.03°–46° and 65.03°–79.84°, which are indexed to, (200), (220), and (311) plans of face center cubic structure of biosynthesized Ag NPs confirmed by using software PANalytical X'Pert [35]. These data are matched with the Joint Committee on Powder Diffraction Standards (JCPDS) file number 03-0921.

The average grain size of Ag<sub>2</sub>O NPs formed in the process can be estimated from the Debye–Scherer equation  $D = K(\lambda/\beta_{1/2})\cos\theta$  by determining the width of (111) Bragg's reflection, where  $K$  is the shape constant,  $\lambda$  is wavelength of the X-ray, and  $\beta_{1/2}$  is the half-width of the peak [10]. In accordance with the report of different studies, the estimated mean size of the particle is found in the range of 4 nm to 6.2 nm.

**3.5. Morphology.** Transmission electron microscopy (TEM) (Figures 7(a) and 7(b)) and scanning electron microscopy (SEM) (Figure 8) are the most widely used microscopic techniques to provide information regarding topography,

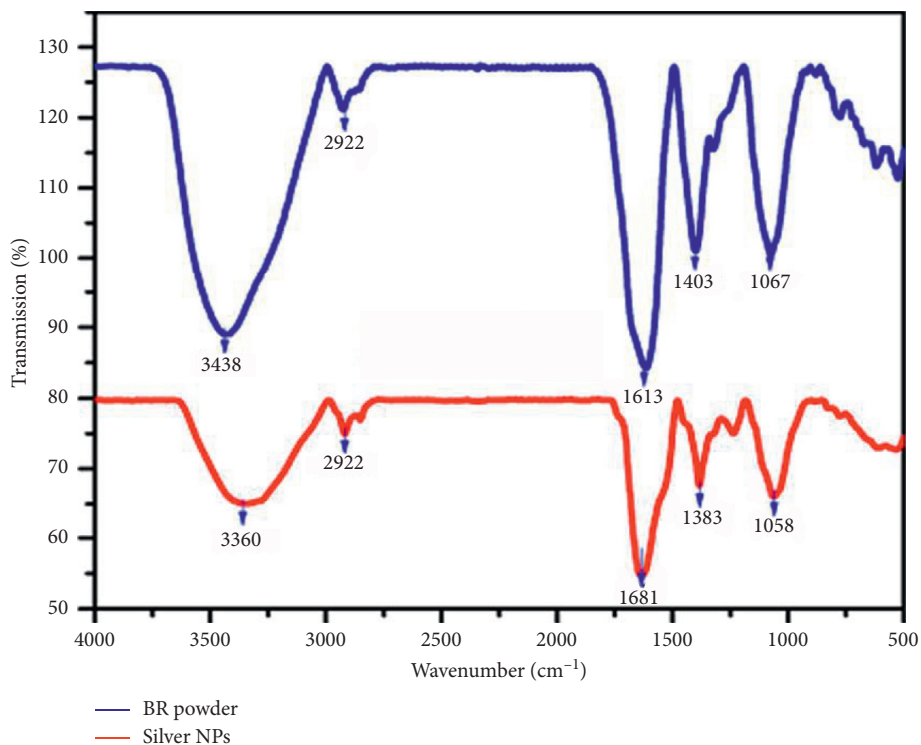


FIGURE 5: FTIR spectra of extract and Ag<sub>2</sub>O NPs [27].

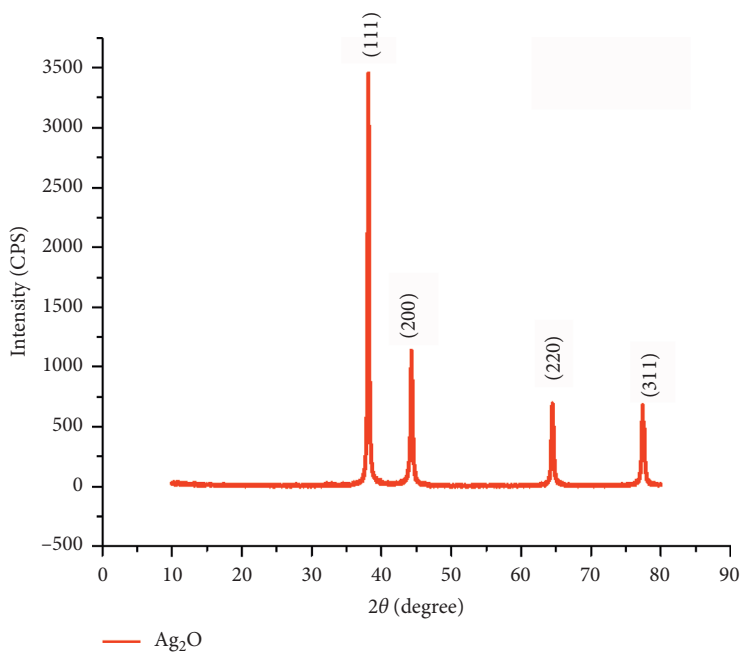


FIGURE 6: XRD pattern of synthesized Ag<sub>2</sub>O nanoparticles [34].

morphology, disparity, shape, size, composition, and crystallography of the sample [13, 37]. As shown in the images of TEM and SEM, most of the green synthesized Ag<sub>2</sub>O NPs are almost spherical shaped while some of the others are elliptical in shape with the size range of ~50 nm. These results are in accordance with the results of many literatures

[7, 10, 26, 28, 36]. The particle size distribution chart (Figure 7(c)) shows the synthesized nanoparticle having size range from ~10 to 90 nm with average diameter of about 45 nm.

The bright circular spots shown in the selected area electron diffraction (SAED) patterns (Figure 7(d)) confirm



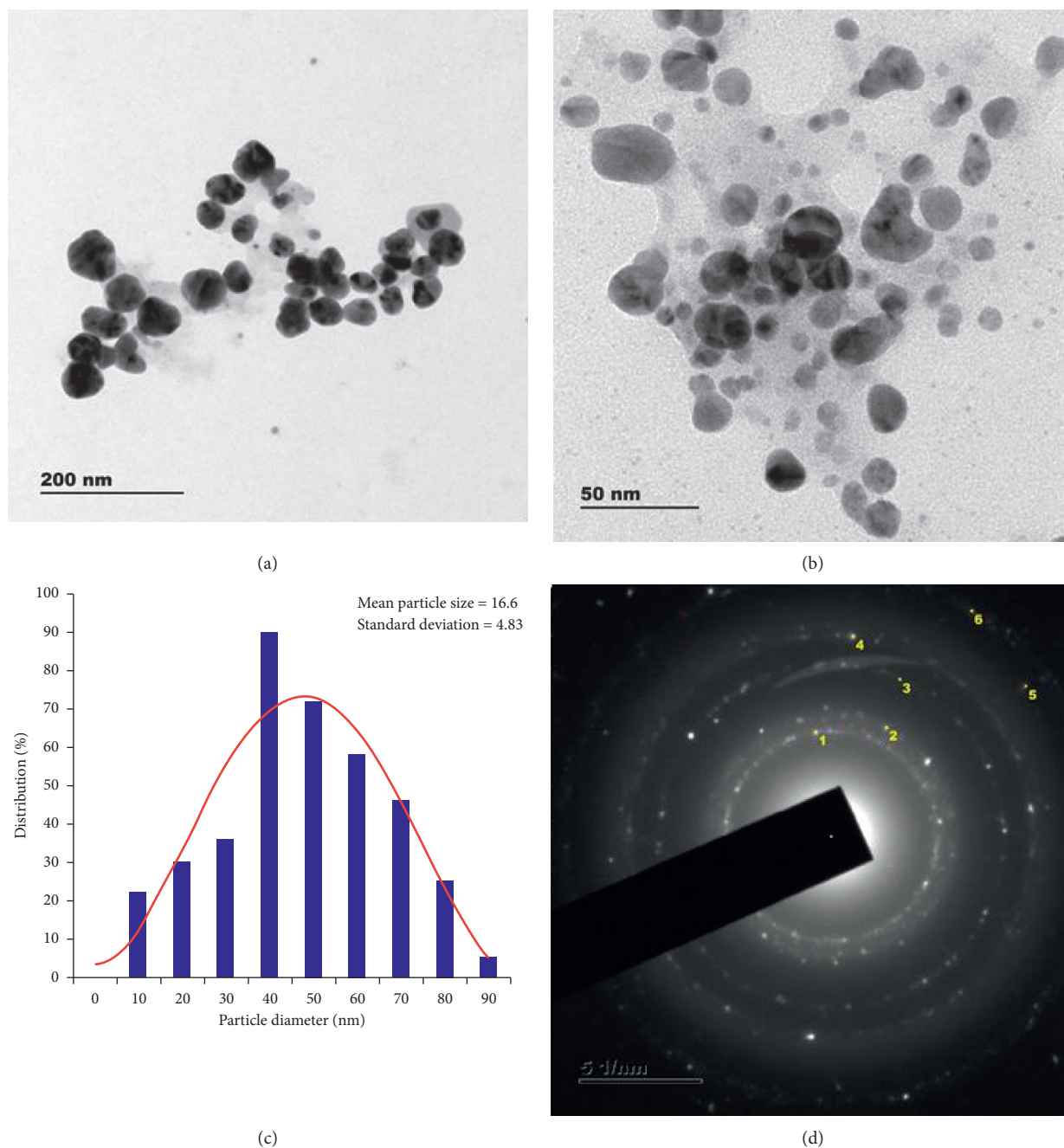


FIGURE 7: TEM images (a and b), particle size histogram (c), and corresponding SAED pattern (d) of  $\text{Ag}_2\text{O}$  NPs [10, 13].

the crystalline nature of  $\text{Ag}_2\text{O}$  NPs [10]. Due to the presence of both individual and agglomerated  $\text{Ag}_2\text{O}$  NPs some of the nanoparticles do not have a smooth surface morphology [25].

#### 4. Photocatalytic Activity of $\text{Ag}_2\text{O}$ NPs

For healthy environment, it is very important to maintain the ecological balance, in which controlling the environmental toxic pollutants is of great importance. Accordingly, it is a credible contribution of researchers towards the healthier environment to organize a setup for the

photocatalytic activity for removal and detection of health hazardous compound from environment as well remediation of water by using semiconductor metal oxide. As reported by different researchers  $\text{Ag}_2\text{O}$  is an effective photocatalytic semiconductor for degradation of different organic pollutants. The stability of  $\text{Ag}_2\text{O}$  NPs was found to be relatively long degradation time of 160 min [22]. These results confirm the fabricated Ag as  $\text{Ag}_2\text{O}$  have high photocatalysts efficiency, which decomposed MO in 10 min under visible light irradiation [38]. Jiang et al. also reported a new use of  $\text{Ag}_2\text{O}$  semiconductor, which exhibits fast photocatalytic performance to decompose MO in 120 sec. and

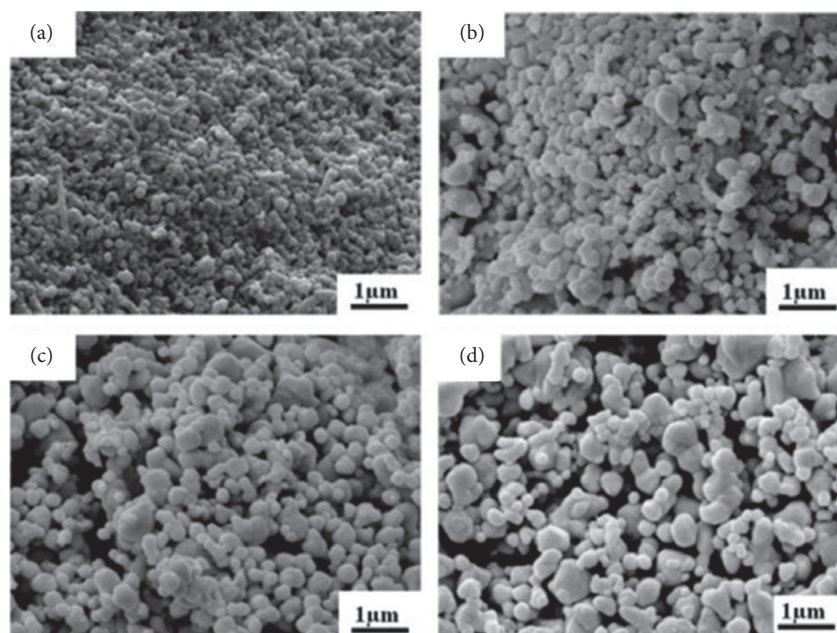


FIGURE 8: Scanning electron microscope (SEM) images of  $\text{Ag}_2\text{O}$  NPs [36].

excellent stability under visible and near-infrared light [7]. Saha et al. investigated the complete photocatalytic degradation of Methyl Blue (MB) within 10 min by using  $\text{Ag}_2\text{O}$  NPs synthesized from fruit extract of *G. arborea* [4].

Jiang et al. [39] studied the photocatalytic application the four silver chalcogen compounds,  $\text{Ag}_2\text{O}$ ,  $\text{Ag}_2\text{S}$ ,  $\text{Ag}_2\text{Se}$ , and  $\text{Ag}_2\text{Te}$ , under visible light. In this work, they analyzed the relationship between the electronic structures and photocatalytic performance and energetic structure of these compounds by means of simulation and experiments. The results of this analysis showed that all the four chalcogenides exhibited interesting photocatalytic activities under ultraviolet, visible, and near-infrared light. However, their photocatalytic performances and stability significantly depended on the band gap width and the valence band and conduct band position, which was determined by their composition. They suggested that increasing the  $X$  atomic number from O to Te resulted in the upward movement of the valence band top and the conduct band bottom, which resulted in narrower band gaps, a wider absorption spectrum, a weaker photooxidization capacity, a higher recombination probability of hole and electron pairs, lower quantum efficiency, and worse stability. Among them, the widest band gap and lowest position of VB and CB in  $\text{Ag}_2\text{O}$  resulted in the highest photocatalytic performance and stability, providing a promising photocatalyst that operated under a sufficiently wide spectrum ( $\text{Ag}_2\text{O} > \text{Ag}_2\text{S} > \text{Ag}_2\text{Se} > \text{Ag}_2\text{Te}$ ).

Bi et al. [40] investigated the photocatalytic degradation of non-AZO dyes over  $\text{Ag}_2\text{O}$  and its acceleration by the addition of an AZO dye under visible light. In this study, they revealed that upon addition of methyl orange, the time taken for the photodegradation of rhodamine B and methylene blue was significantly shortened from 50 to 18 min and from 20 to 8 min, respectively. The results of this

study indicated that this acceleration can be ascribed to the synergistic effect of the  $\text{Ag}_2\text{O}$  and AZO species. Based on the results of this work the researchers confirmed  $\text{Ag}_2\text{O}$  to be an excellent visible light driven photocatalyst for wastewater treatment. Thus this interesting phenomenon is useful for the application of  $\text{Ag}_2\text{O}$  as photocatalyst to treat real wastewater and could promote the practicability of photocatalytic technology for environmental protection.

All these results are informed as to generalize as both the chemical and green synthesized  $\text{Ag}_2\text{O}$  NPs exhibit excellent catalytic performance for the degradation of harmful organic compounds. The results of all these studies conclude that  $\text{Ag}_2\text{O}$  has excellent performance and high stability for photocatalytic degradation of organic pollutants and dyes.

In this work Methylene orange was selected as the reference compound for photodecomposition to evaluate the photocatalytic performance of  $\text{Ag}_2\text{O}$ . The removal rates of MO from aqueous solution under visible light illumination in  $\text{Ag}_2\text{O}$  nanostructures and other photocatalysts used as the comparison including N-TiO<sub>2</sub> were investigated to exclude the interference of adsorption in determining photocatalytic activity [22]. The degradation rate was calculated by pseudo-first-order kinetic model due to the low initial concentrations of the reactants using the following equation:fd3

$$\text{decolorization rate} = \ln \frac{C_0}{C} = kKt = k_{\text{app}}t, \quad (3)$$

where  $k_{\text{app}}$  is the apparent first-order rate constant ( $\text{min}^{-1}$ ) [41].

The decolorization of MO gradually decreased in the presence of  $\text{Ag}_2\text{O}$  nanoparticle with the increment of the exposed time, indicating a decrease in dye concentration. This result clearly shows that in the presence of  $\text{Ag}_2\text{O}$  nanostructures as a photocatalyst, MO degraded to 100%

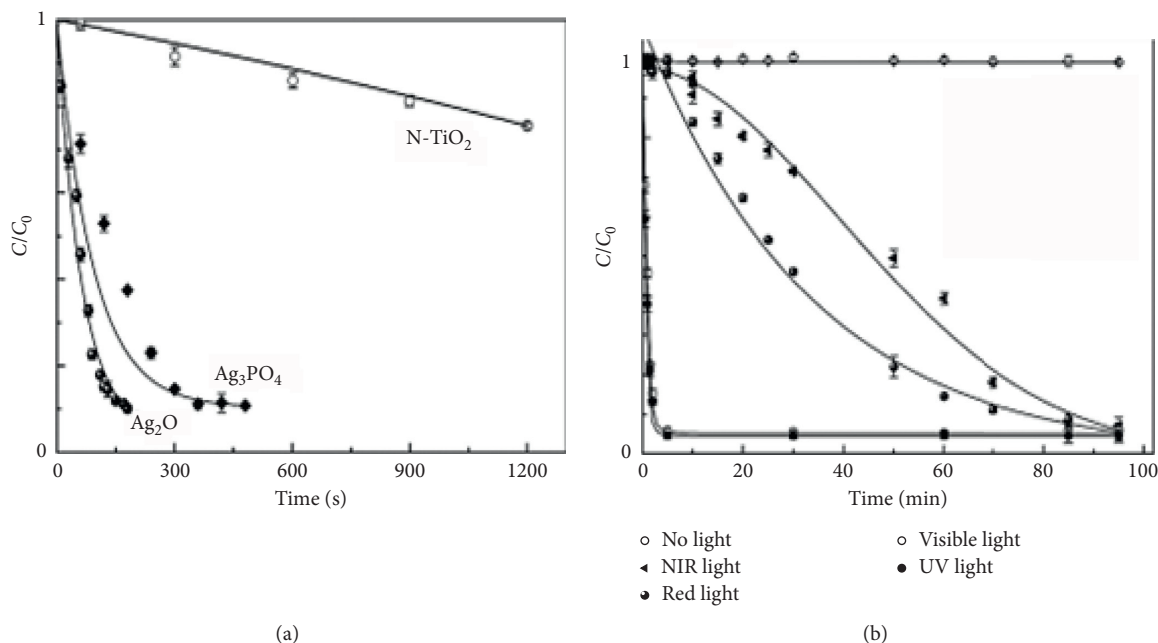


FIGURE 9: (a) Photocatalytic activity of Ag<sub>2</sub>O, Ag<sub>3</sub>PO<sub>4</sub>, and N-TiO<sub>2</sub>. (b) The effect of light source on photocatalytic activity of Ag<sub>2</sub>O NPs [7].

within 160 min under visible light irradiation which was faster than N-TiO<sub>2</sub>, tested under identical experimental conditions for the photocatalytic activity comparison. To exclude the effect of other factors on the photocatalytic activity of Ag<sub>2</sub>O, control experiments were designed as follows: under dark conditions with Ag<sub>2</sub>O powder, the concentration of MO did not change over time.

The above results strongly agree with the results reported by Jiang et al., who used Ag<sub>2</sub>O to exhibit fast photocatalytic degradation of MO (Figure 9(a)) and confirmed the photocatalytic activities of Ag<sub>2</sub>O decrease with increasing the wavelength of light (from UV to near IR) (Figure 9(b)) [7].

Jiang et al. [42] studied the preparation of a magnetically separable photocatalyst, Fe<sub>3</sub>O<sub>4</sub>-SiO<sub>2</sub>-APTES-Ag<sub>2</sub>O nanocomposite, and evaluated its photocatalytic performance under visible light. Results of this study show that the obtained exhibited high photocatalytic activity for organic pollutants under visible light irradiation, highly efficient separation and recovery, and excellent stability after recycling and also equivalent photocatalytic performance to the pure Ag<sub>2</sub>O under visible light irradiation and sunlight. Phenol and methyl orange can be effectively photodegraded with the composite catalyst in 10 min. The results reported by Jiang et al. (Figure 9(a)) showed the fast decomposition of MO with Ag<sub>2</sub>O, homemade Ag<sub>3</sub>PO<sub>4</sub>, and N-doped TiO<sub>2</sub> photocatalyst under visible light irradiation which from the results of this study Jiang et al. suggested that Ag<sub>2</sub>O eliminated the dye completely within a short period of time as compared with the other two photocatalysts (Ag<sub>3</sub>PO<sub>4</sub> and N-doped TiO<sub>2</sub>) under similar conditions.

**4.1. Photo Degradation Products of MO with Ag<sub>2</sub>O NPs.** Figure 10 showed the full UV-visible spectrum of MO solution at different photodecomposition time. The typical

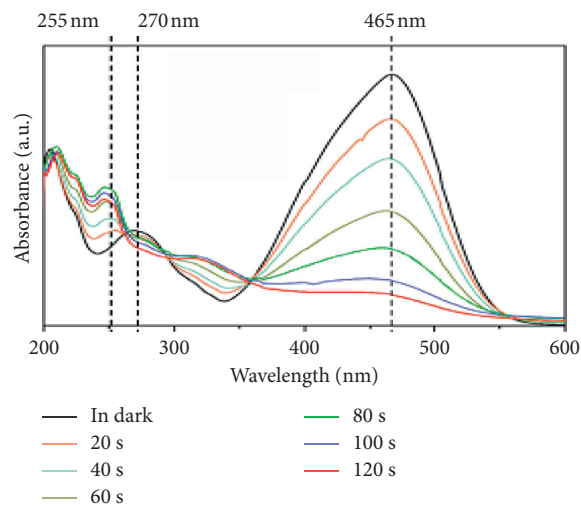


FIGURE 10: UV-Vis spectrum of MO solution in photodegradation process [7].

peaks observed at 465 nm and 270 nm are a typical absorption peak of MO solution, the AZO structure, and benzene ring conjugate structure, respectively. A rapid decrement of AZO group peak confirmed that the complete destroying of chromophoric group is found in MO by means of photocatalyst (Ag<sub>2</sub>O) [7]. In general, the result of this study confirmed as Ag<sub>2</sub>O is a strong photocatalyst, which mineralized MO completely in a short time interval.

**4.2. Photocatalytic Process Mechanism.** The working mechanism of Ag<sub>2</sub>O is conjectured and described in Figure 11. The band gap energy of Ag<sub>2</sub>O is reported to be ~1.3 eV with an energy level of the CB edge of +0.2 eV

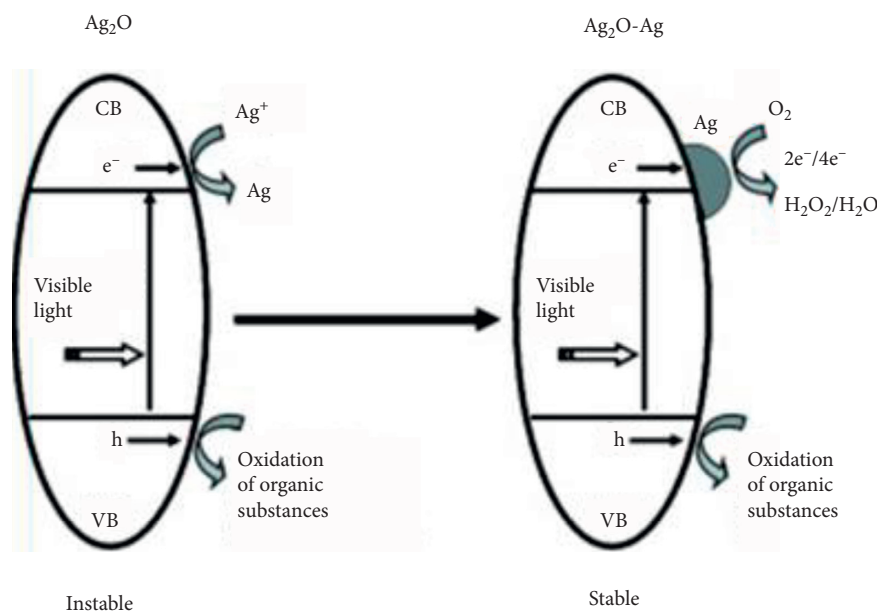
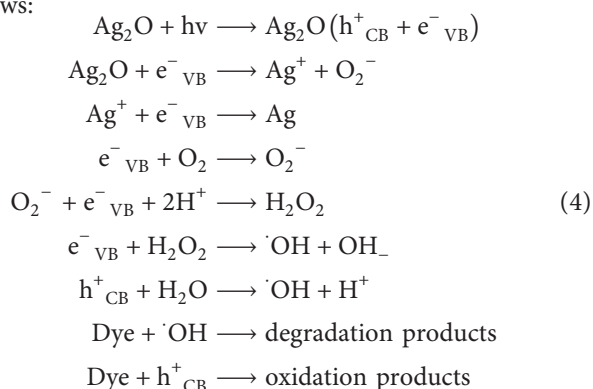


FIGURE 11: Schematic diagrams showing the self-stabilizing process of  $\text{Ag}_2\text{O}$  photocatalyst under visible light irradiation: (left) photo-generated electrons are captured by  $\text{Ag}^+$  ions on the as-prepared  $\text{Ag}_2\text{O}$ ; (right) photogenerated electrons are captured by  $\text{O}_2$  through metallic Ag, which is formed during the initial light irradiation of fresh  $\text{Ag}_2\text{O}$  ( $h^+$  = holes and  $e^-$  = electrons) [22].

(vs. SHE) [5]. When the  $\text{Ag}_2\text{O}$  photocatalyst is irradiated with visible light, the photogenerated electrons are produced in the CB while photogenerated holes ( $h^+$ ) remain in the VB. In view of the more positive potential of  $\text{Ag}^+/\text{Ag}$  (0.7991 V vs. SHE) compared with  $\text{O}_2/\text{H}_2\text{O}$  (0.046 V vs. SHE), the photogenerated electrons are preferably transferred to the lattice  $\text{Ag}^+$ . Actually, the  $\text{Ag}^+$  ion has been demonstrated to be an effective sacrificial reagent to capture photogenerated electrons for the evolution of oxygen during the splitting of water [7]. The photocatalytic process mechanism of  $\text{Ag}_2\text{O}$  for degradation of organic compounds can be described as follows:



After absorbing photons in  $\text{Ag}_2\text{O}$ , photogenerated electrons in the CB are captured by  $\text{Ag}^+$  ions to form Ag clusters [43]. Apparently, the photogenerated holes in  $\text{Ag}_2\text{O}$  have a strong oxidation power to oxidize the lattice  $\text{O}_2$  in  $\text{Ag}_2\text{O}$ . The binding energy of each Ag cluster relative is to the excitation energy. This indicates that  $\text{Ag}_2\text{O}$  has a great potential to be used as a stable and highly efficient photocatalyst for photocatalytic decomposition of organic contaminants under visible light irradiation [22].

**4.3. Stability of Silver Oxide for Photocatalytic Application.** It is interesting and important to consider how  $\text{Ag}_2\text{O}$  can act as a stable and efficient photocatalyst under visible light irradiation. To achieve efficient and durable photocatalysis, photocatalysts must have effective and broad spectrum light absorption and rapid charge separation [8]. Both workers, Jiang et al. [7] showed how  $\text{Ag}_2\text{O}$  can act as a stable and efficient photocatalyst under visible light irradiation by repeated photocatalytic decolonization of MO as shown in Figures 11 and 12, respectively.

Wang et al. (2011) reported the stability of silver oxide for photocatalytic application as the partial content of  $\text{Ag}^+$  in  $\text{Ag}_2\text{O}$  was reduced in situ by photogenerated electrons and formed metallic Ag during the first cycle of photocatalytic experiments (Figure 10, left).

Once a certain amount of metallic Ag is formed on the surface of  $\text{Ag}_2\text{O}$ , the following photogenerated electrons tend to transfer to the metallic Ag sites and are then captured by oxygen (Figure 10, right). Considering a more positive potential (+0.2 eV vs. SHE) of the CB level of  $\text{Ag}_2\text{O}$  compared with the single electron reduction of oxygen ( $\text{O}_2 + e + \text{H}^+ \longrightarrow \text{H}_2\text{O}_2(\text{aq})$ , 0.046 V vs. SHE), it is possible that the metallic Ag works as an electron pool and transfers the photogenerated electrons to oxygen through multi-electron-transfer [22]. Previous research results also demonstrated that the noble metal Pt loaded on the surface of  $\text{WO}_3$  could work as effective multi-electron-transfer active sites for oxygen reduction [41, 42].

For the photogenerated holes, it is the organic substances that are preferably oxidized on the surface of  $\text{Ag}_2\text{O}$ , instead of lattice oxygen in  $\text{Ag}_2\text{O}$ , resulting in the enhanced stability of the  $\text{Ag}_2\text{O}$ -Ag crystal structure (Figure 11). The above results highlight an interesting self-stability mechanism for the photosensitive  $\text{Ag}_2\text{O}$  by in situ photogenerated Ag,

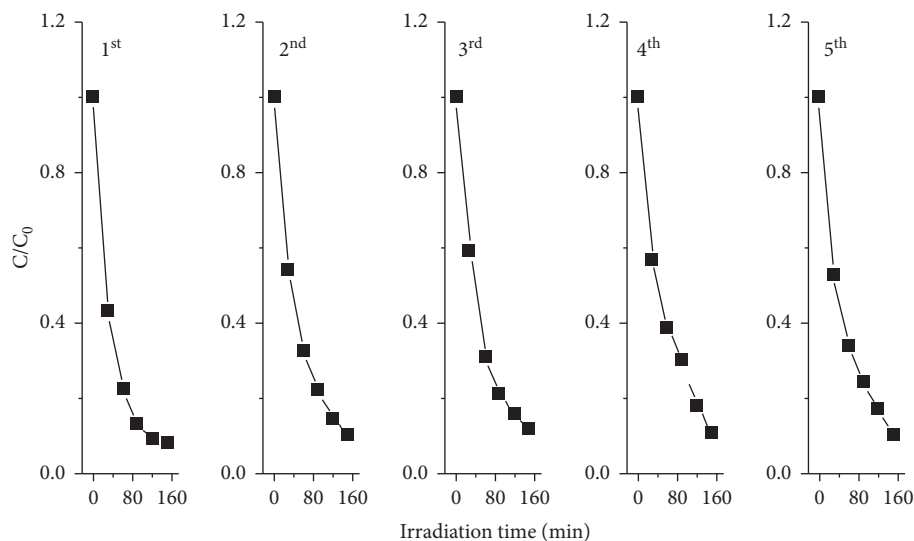


FIGURE 12: Repeated photocatalytic decolorization experiments of MO over the  $\text{Ag}_2\text{O}$  photocatalyst under visible light irradiation [22].

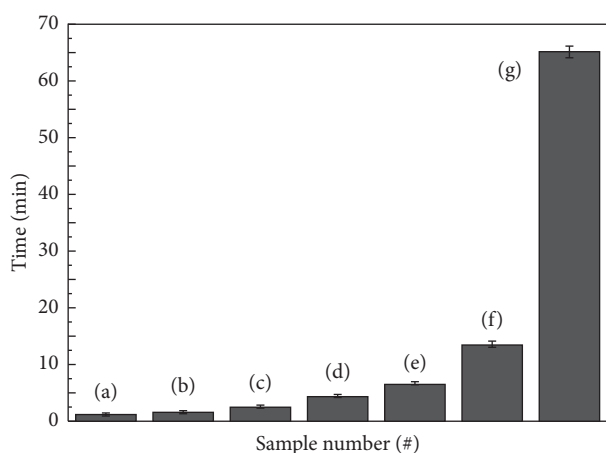


FIGURE 13: Reacting time for reaching 90% MO degradation rate with different samples: (a) fresh sample, (b) 3-cycle sample, (c) 8-cycle sample, (d) 24 h exposed sample under sunlight in air, (e) 24 h exposed sample under sunlight in water, (f) fresh  $\text{Ag}_3\text{PO}_4$ , and (g) fresh  $\text{N-TiO}_2$  activity [7].

arising from the partial photodecomposition of  $\text{Ag}_2\text{O}$ . Actually, the self-stability mechanism is not just restricted to  $\text{Ag}_2\text{O}$  photocatalysts [44]. Cao et al. found that Ag species were formed on AgBr in the early stage of the photocatalysis of the  $\text{CH}_3\text{OH}/\text{H}_2\text{O}$  solution and AgBr is not destroyed under successive UV irradiation [6]. Similarly, Ag/AgCl [45] and Ag/AgBr, [6] have been demonstrated to be efficient and stable visible light photocatalysts. Those facts strongly support that the structure stability of Ag-based photosensitive materials can be markedly enhanced by metallic Ag.

The biosynthesized  $\text{Ag}_2\text{O}$  has a greater stability to the photocatalytic decolorization of organic dyes more than five times under the exposure of UV-light [7, 22]. The corresponding results shown in Figures 12 and 13, respectively, confirmed that although the photocatalytic activity of

repeated cycles is slightly decreased compared with the first-cycle result,  $\text{Ag}_2\text{O}$  can maintain a stable and efficient photocatalytic performance after the first-cycle test. Based on these results we can conclude that  $\text{Ag}_2\text{O}$  NP is a highly stable photocatalyst used after repeated using for degradation of harmful organic compounds efficiently within a few minutes, better than that of other common photocatalysts like  $\text{Ag}_3\text{PO}_4$  or  $\text{N-TiO}_2$  [7].

According to these observations, although the photocatalytic activity of repeated cycles was slightly decreased compared with the first-cycle result,  $\text{Ag}_2\text{O}$  can maintain a stable and efficient photocatalytic performance after the first-cycle test.

## 5. Conclusions

Green synthesis method is an appropriate method to synthesize metal oxide nanostructures with efficient yield. The past studies revealed that  $\text{Ag}_2\text{O}$  nanostructures can be effectively synthesized by using silver nitrate as the starting reagent through the biosynthesis method as confirmed by the microscopic (SEM and TEM) and spectroscopic (XRD, XPS, EDS, UV-Vis, and FT-IR) results. The green synthesized nanocrystalline  $\text{Ag}_2\text{O}$  efficiently decolorize or mineralize toxic organic pollutants after irradiation of visible light for a few time. This confirmed that green synthesized  $\text{Ag}_2\text{O}$  nanoparticles are good, highly efficient, and stable photocatalysts for degrading harmful organic compounds and dyes with visible light irradiation.

Even though a significant progress is being made toward the development of visible light activated  $\text{Ag}_2\text{O}$  nanoparticles, the environmental fate and toxicity of  $\text{Ag}_2\text{O}$  are critical issues during their design for different applications because overdose of silver oxide causes argyria, carcinogenic, inhibits "good bacteria," prevents photosynthesis in algae, and so forth. Thus, further studies need to develop

environmentally acceptable, biocompatible, and cost-effective synthetic approaches for Ag<sub>2</sub>O nanoparticle.

## Conflicts of Interest

The authors declare that they have no conflicts of interest.

## Acknowledgments

Workneh M. Shume, H.C. Ananda Murthy, and Enyew Amare Zereffa are grateful to Adama Science and Technology University, Ethiopia, for rendering support towards publication of this work.

## References

- [1] R. P. Feynman, "There's plenty of room at the bottom," *Engineering and Science*, vol. 23, no. 5, pp. 22–36, 1960.
- [2] P. Sevilla, "Molecular characterization of drug's nanocarriers based on plasmon-enhanced spectroscopy: fluorescence (SEF) and Raman (SERS)," *Optica Pura Y Aplicada*, vol. 46, no. 2, pp. 111–119, 2013.
- [3] C. Burda, X. Chen, R. Narayanan, and M. A. El-sayed, "Chemistry and properties of nanocrystals of different shapes," *Chemical Reviews*, vol. 105, no. 4, pp. 1025–1102, 2005.
- [4] J. Saha, A. Begum, A. Mukherjee, and S. Kumar, "A novel green synthesis of silver nanoparticles and their catalytic action in reduction of Methylene Blue dye," *Sustainable Environment Research*, vol. 27, no. 5, pp. 245–250, 2017.
- [5] H. Xue, K. Wang, Y. Bai et al., "Preparation of novel Ag<sub>2</sub>O/Na<sub>3</sub>Bi(PO<sub>4</sub>)<sub>2</sub> heterogeneous nanostructures with enhanced visible-light responsive photocatalytic activity," *Materials Letters*, vol. 242, pp. 39–41, 2019.
- [6] J. Cao, B. Luo, H. Lin, and S. Chen, "Photocatalytic activity of novel AgBr/WO<sub>3</sub> composite photocatalyst under visible light irradiation for methyl orange degradation," *Journal of Hazardous Materials*, vol. 190, no. 1–3, pp. 700–706, 2011.
- [7] W. Jiang, X. Wang, Z. Wu et al., "Silver oxide as superb and stable photocatalyst under visible and near-infrared light irradiation and its photocatalytic mechanism," *Industrial & Engineering Chemistry Research*, vol. 54, no. 3, pp. 832–841, 2015.
- [8] Y. Li, Q. Wang, H. Wang, J. Tian, and H. Cui, "Novel Ag<sub>2</sub>O nanoparticles modified MoS<sub>2</sub> nanoflowers for piezoelectric-assisted full solar spectrum photocatalysis," *Journal of Colloid and Interface Science*, vol. 537, pp. 206–214, 2019.
- [9] A. Hernández-Ramírez and I. Medina-Ramírez, *Photocatalytic Semiconductors Synthesis, Characterization, and Environmental Applications*, Springer, Berlin, Germany, 2014.
- [10] V. Manikandan, "Green synthesis of silver oxide nanoparticles and its antibacterial activity against dental pathogens," *3 Biotech*, vol. 7, no. 1, 2017.
- [11] M.-J. Kim, S.-H. Kim, H.-Y. Park, and Y.-D. Huh, "Morphological evolution of Ag<sub>2</sub>O microstructures from cubes to octapods and their antibacterial activities," *Bulletin of the Korean Chemical Society*, vol. 32, no. 10, pp. 3793–3795, 2011.
- [12] M. Yadav, "Biological synthesis and antibacterial activity of silver oxide nanoparticle prepared from *Carica papaya* root extract," *International Journal of Pure & Applied Bioscience*, vol. 6, no. 2, pp. 1632–1639, 2018.
- [13] A. A. Rokade, M. P. Patil, S. I. Yoo, W. K. Lee, and S. S. Park, "Pure green chemical approach for synthesis of Ag<sub>2</sub>O nanoparticles," *Green Chemistry Letters and Reviews*, vol. 9, no. 4, pp. 216–222, 2016.
- [14] S. Rajakannu, S. Shankar, S. Perumal, and S. Subramanian, "Biosynthesis of silver nanoparticles using *Garcinia mangostana* fruit extract and their antibacterial, antioxidant activity," *International Journal of Current Microbiology and Applied Sciences*, vol. 4, no. 1, pp. 944–952, 2015.
- [15] U. G. Akpan and B. H. Hameed, "Parameters affecting the photocatalytic degradation of dyes using TiO<sub>2</sub>-based photocatalysts: a review," *Journal of Hazardous Materials*, vol. 170, no. 2–3, pp. 520–529, 2009.
- [16] A. Cassano, R. Dillert, R. Goslich, O. Alfano, and D. Bahnemann, "Photocatalysis in water environments using artificial and solar light," vol. 58, no. 2–3, pp. 199–230, 2002.
- [17] P. Kumar, M. Govindaraju, S. Senthamilselvi, and K. Premkumar, "Photocatalytic degradation of methyl orange dye using silver (Ag) nanoparticles synthesized from *Ulva lactuca*," *Colloids and Surfaces B: Biointerfaces*, vol. 103, pp. 658–661, 2013.
- [18] Y. He, F. Grieser, and M. Ashokkumar, "The mechanism of sonophotocatalytic degradation of methyl orange and its products in aqueous solutions," *Ultrasonics Sonochemistry*, vol. 18, no. 5, pp. 974–980, 2011.
- [19] T. Welderfael, O. P. Yadav, A. M. Tadesse, and J. Kaushal, "Synthesis, characterization and photocatalytic activities of Ag-N-Codoped ZnO nanoparticles for degradation of methyl red," *Bulletin of the Chemical Society of Ethiopia*, vol. 27, no. 2, pp. 221–232, 2013.
- [20] W. Wei, X. Mao, L. A. Ortiz, and D. R. Sadoway, "Oriented silver oxide nanostructures synthesized through a template-free electrochemical route," *Journal of Materials Chemistry*, vol. 21, no. 2, pp. 432–438, 2011.
- [21] N. L. Yong, A. Ahmad, and A. W. Mohammad, "Synthesis and characterization of silver oxide nanoparticles by a novel method," *International Journal of Scientific and Engineering Research*, vol. 4, no. 5, pp. 155–158, 2013.
- [22] X. Wang, S. Li, H. Yu, J. Yu, and S. Liu, "Ag<sub>2</sub>O as a new visible-light photocatalyst: self-stability and high photocatalytic activity," *Chemistry—A European Journal*, vol. 17, no. 28, pp. 7777–7780, 2011.
- [23] A. K. Ojha, J. Rout, S. Behera, and P. L. Nayak, "Green synthesis and characterization of zero valent silver nanoparticles from the leaf extract of *Datura metel*," *International Journal of Pharmaceutical Research and Allied*, vol. 2, no. 2, pp. 31–35, 2013.
- [24] S. Ravichandran, V. Paluri, G. Kumar, K. Loganathan, and B. R. Kokati Venkata, "A novel approach for the biosynthesis of silver oxide nanoparticles using aqueous leaf extract of *Callistemon lanceolatus* (Myrtaceae) and their therapeutic potential," *Journal of Experimental Nanoscience*, vol. 11, no. 6, pp. 445–458, 2016.
- [25] M. Jalees, "Green synthesis of silver oxide nanoparticles prepared from waste part of mango peels," *International Journal of Pure & Applied Bioscience*, vol. 6, no. 3, pp. 502–508, 2018.
- [26] S. Ahmed, M. Ahmad, B. L. Swami, and S. Ikram, "A review on plants extract mediated synthesis of silver nanoparticles for antimicrobial applications: a green expertise," *Journal of Advanced Research*, vol. 7, no. 1, pp. 17–28, 2016.
- [27] M. Velu, Y. Pyong-In, V. Palanivel et al., "Production, optimization and characterization of silver oxide nanoparticles using *Artocarpus heterophyllus* rind extract and their antifungal activity," *African Journal of Biotechnology*, vol. 16, no. 36, pp. 1819–1825, 2017.

- [28] S. B. Khan, M. M. Rahman, H. M. Marwani, A. M. Asiri, and K. A. Alamry, "Exploration of silver oxide nanoparticles as a pointer of lanthanum for environmental applications," *Journal of the Taiwan Institute of Chemical Engineers*, vol. 45, no. 5, pp. 2770–2776, 2014.
- [29] T. Fafal, P. Taştan, B. S. Tüzün, M. Ozyazici, and B. Kivcak, "Synthesis, characterization and studies on antioxidant activity of silver nanoparticles using *Asphodelus aestivus* Brot. aerial part extract," *South African Journal of Botany*, vol. 112, pp. 346–353, 2017.
- [30] W. H. Bragg, "X rays and crystals," *Nature*, vol. 90, no. 1912, p. 219, 1912.
- [31] S. M. Hosseinpour-Mashkani and M. Ramezani, "Silver and silver oxide nanoparticles: synthesis and characterization by thermal decomposition," *Materials Letters*, vol. 130, pp. 259–262, 2014.
- [32] M. J. Hostetler, J. J. Stokes, and R. W. Murray, "Infrared spectroscopy of three-dimensional self-assembled monolayers: *N*-alkanethiolate monolayers on gold cluster compounds," *Langmuir*, vol. 12, no. 15, pp. 3604–3612, 1996.
- [33] B. D. Hall, D. Zanchet, and D. Ugarte, "Estimating nanoparticle size from diffraction measurements," *Journal of Applied Crystallography*, vol. 33, no. 6, pp. 1335–1341, 2000.
- [34] Z. H. Dhoondia and H. Chakraborty, "Lactobacillus mediated synthesis of silver oxide nanoparticles," *Nanomater. Nanotechnol*, vol. 2, no. 15, 2013.
- [35] M. Imran Din and A. Rani, "Recent advances in the synthesis and stabilization of nickel and nickel oxide nanoparticles: a green adeptness," *International Journal of Analytical Chemistry*, vol. 2016, Article ID 3512145, 14 pages, 2016.
- [36] R. Rajakumari, C. Priya, and A. Srilekha, "Synthesis and characterization of nano  $\text{Ag}_2\text{O}$  and  $\text{Cu}(\text{OH})_2$  by solution reduction method and their antibacterial studies," *Journal of Nanoscience and Technology*, vol. 4, no. 4, pp. 435–438, 2018.
- [37] C.-M. Li, I. M. Robertson, M. L. Jenkins, J. L. Hutchison, and R. C. Doole, "In situ TEM observation of the nucleation and growth of silver oxide nanoparticles," *Micron*, vol. 36, no. 1, pp. 9–15, 2005.
- [38] G. Wang, X. Ma, B. Huang et al., "Controlled synthesis of  $\text{Ag}_2\text{O}$  microcrystals with facet-dependent photocatalytic activities," *Journal of Materials Chemistry*, vol. 22, no. 39, pp. 21189–21194, 2012.
- [39] W. Jiang, Z. Wu, Y. Zhu, W. Tian, and B. Liang, "Systematic research on  $\text{Ag}_2\text{X}$  (X=O, S, Se, Te) as visible and near-infrared light driven photocatalysts and effects of their electronic structures," *Applied Surface Science*, vol. 427, pp. 1202–1216, 2018.
- [40] N. Bi, H. Zheng, Y. Zhu, W. Jiang, and B. Liang, "Visible-light-driven photocatalytic degradation of non-azo dyes over  $\text{Ag}_2\text{O}$  and its acceleration by the addition of an azo dye," *Journal of Environmental Chemical Engineering*, vol. 6, no. 2, pp. 3150–3160, 2018.
- [41] J. Ahmad and K. Majid, "In-situ synthesis of visible-light responsive  $\text{Ag}_2\text{O}$ /graphene oxide nanocomposites and effect of graphene oxide content on its photocatalytic activity," *Advanced Composites and Hybrid Materials*, vol. 1, no. 2, pp. 374–388, 2018.
- [42] W. Jiang, F. Sun, Y. Zeng et al., "Preparation and application of separable magnetic  $\text{Fe}_3\text{O}_4\text{-SiO}_2\text{-APTES-Ag}_2\text{O}$  composite particles with high visible light photocatalytic performance," *Journal of Environmental Chemical Engineering*, vol. 6, no. 1, pp. 945–954, 2018.
- [43] R. Tanaka, S. Takata, M. Katayama et al., "Photocatalytic synthesis of silver-oxide clathrate  $\text{Ag}_7\text{O}_8\text{NO}_3$ ," *Journal of The Electrochemical Society*, vol. 157, no. 12, p. E181, 2010.
- [44] C. An, S. Wang, Y. Sun et al., "Plasmonic silver incorporated silver halides for efficient photocatalysis," *Journal of Materials Chemistry A*, vol. 4, no. 12, pp. 4336–4352, 2016.
- [45] D. Xu, W. Shi, C. Song et al., "In-situ synthesis and enhanced photocatalytic activity of visible-light-driven plasmonic  $\text{Ag/AgCl/NaTaO}_3$  nanocubes photocatalysts," *Applied Catalysis B: Environmental*, vol. 191, pp. 228–234, 2016.